Impact of Extraction Method on the Properties of Polymer Composites Reinforced with Natural Fiber from Agave Americana L

Afef Mansouri
afeffmansouri@gmail.com

University of Sfax
Jalel Ben Nasr
University of Gabes
Fatma Hentati
National Engineering School of Tunis ENIT
Mohamed Ben Amar
University of Sfax

Research Article

Keywords: Agave Americana L, Naturel fiber, Polymer composites, Compression molding, Flexural and Modulus Strength, SEM, EDX

Posted Date: March 22nd, 2024

DOI: https://doi.org/10.21203/rs.3.rs-4131827/v1

Additional Declarations: No competing interests reported.

Abstract

In this study, we introduce a novel extraction technique involving burying lignocellulosic fibers from the leaves of Agave Americana L in soil. These fibers are then used to reinforce a polymer epoxy, aiming to enhance the mechanical and physical properties of the composite material. The aim is to valorize Agave Americana L, which is abundant and available in large quantities in Tunisia. The fiber content for the composites was chosen (0%, 10%, and 20%) to enhance the properties of the polymer composite. The mechanical, physical, and morphological properties of the composites were evaluated using SEM and EDX. Results showed that the flexural properties of the composites, based on biological and raw fibers (RFE10, FE10, RFE20, and BFE20), increased with the higher content of agave fibers. Furthermore, the mechanical findings revealed flexural strength varying between 141.74 and 161.92 MPa, and a modulus strength ranging between 8902 and 13674 MPa for biological fiber weights of 10% and 20%, respectively.

1. Introduction

Due to the increasing environmental threats and pollution resulting from the use of plastics and synthetic materials, the focus in materials science has shifted towards the development of biodegradable material sources. Bio-composites play a crucial role in creating biodegradable materials that not only meet design requirements but also align with customer preferences. The production of bio-composites is environmentally friendly and biodegradable, making them a more suitable alternative to products made from synthetic materials (Estaji et al. 2021)(Mousavi et al. 2021b)(Razavi et al. 2022)(Mousavi et al. 2021a) .

Many researchers opt for lignocellulosic fibers, as they are sustainable, non-toxic, inexpensive, and possess satisfactory mechanical and physical properties. Composites consisting of agave fibers and polymer matrices have gained recent attention in industries such as automotive, aerospace, and construction, particularly in molded applications where safety is a priority. Various types of fibers, including synthetic and cellulosic fibers, are employed to reinforce high-strength composites.

Synthetic fibers are most commonly used because of their low cost and special mechanical properties, but because of the negative environmental and health impacts, which are also very expensive, the production of these fibers requires a lot of energy (Labidi et al. 2019). These various problems limit the use of these fibers as reinforcement in polymers and draw the attention of many researchers to the use of lingo cellulose fibers. These various problems limit the use of these fibers as reinforcement in polymers and draw the attention of many researchers to the use of lingo cellulose fibers. Due to the availability of lignocellulosic fibers in large quantities worldwide and offer many advantages such as biodegradability, recyclability, lower cost, low density, non-toxicity, renewability of the resource, good thermal and mechanical properties, and lower environmental impact (Rosli et al. 2015). The lignocellulosic fibers used in this study were obtained from Agave Americana L. leaf. Common names of Agave americana are: aloe americana or century plant and maguey. Agave belongs to the monocotyledonous family called Agave (Hulle et al. 2015). The plant flourishes in South Africa as well as the Mediterranean area (Msahli et al. 2005). In Tunisia, the Agave Americana is the most abundant variety of agave. This variety is characterized by the fact that it is a voluminous plant and rigid due to the existence of lignin on its surface (Bouaziz et al. 2014; Hulle et al. 2015). The color of the fiber varies from milky white to golden yellow. The fibers Agave can be extracted by several methods such as mechanical (el Oudiani et al. 2008), chemical, biological (use of bacteria and enzymes) (Bessadok et al. 2009), and retting in water (Mylsamy and Rajendran 2011a). The traditional method, named retting in seawater consists in putting the Agave leaves in seawater for a period varying between 3–6 weeks. This method leads to obtain fibers. Asma and al used this extraction method (retting in seawater) in their works (Bessghaier and Oudiani 2010). Mylsamy and al. have extracted fibers by this method for elaboration composite (Mylsamy and Rajendran 2011b). Water retting is not environmentally sound at an industrial scale due to the large volume of polluted water corruption, and squandering of water. Also, the unpleasant smell produced by the anaerobic fermentation (Akin et al. 2007), as well the high costs of labor and drying caused by water retting (Henriksson et al. 1997). Also, enzymatic retting hasn't yet reached industry scale due to high costs (Akin 2013).

Agave leaves undergo hydrolysis treatment in an autoclave for 90 minutes at high temperature (120°C) (Jaouadi et al. 2011). However, this process leads to the degradation of the cell wall, which can adversely affect the mechanical properties of the isolated fibers (Bezazi et al. 2014). An alternative extraction method proposed by certain authors involves burying the leaves in soil. However, Bezazi focused solely on the mechanical properties, and the optimization of new extraction methods of Agave fibers after burial in soil for composite production has not been addressed in the literature until now. This study represents the first investigation of its kind worldwide. Previously, the physico-chemical properties of these fibers were published (Mansouri et al. 2020).

The properties of natural fiber-reinforced polymer composites are influenced by various factors, including the extraction method, fiber content, fiber dispersion, fiber orientation, matrix selection, composite manufacturing process, and interfacial strength (Pickering et al. 2016). For instance, Khan et al. studied the fracture behavior of bamboo fiber-reinforced epoxy composites using different fiber lengths. Their findings revealed that composites containing bamboo fibers with lengths of 25 mm and 10 mm exhibited the highest and lowest fracture toughness, respectively (Khan et al. 2017). Singha et al. (Singha and Rana 2012) explored the impact of dimensions (8mm, 3mm, and 90µm particle length) on the mechanical properties of Agave Americana L fiber-reinforced polystyrene composite. The study revealed that particle-reinforced composites exhibited the highest tensile, compressive, and flexural strength. Another investigation by Mylsamy et al. focused on the effect of dimensions (3.7 and 10 mm) on the mechanical properties of epoxy reinforced with Agave Americana L (Mylsamy and Rajendran 2011a). The results demonstrated that the mechanical properties of epoxy reinforced with Agave Americana L were not adversely affected. They found that mechanical properties improved at a length of 3 mm due to enhanced adhesion between the fiber and the matrix.

The objective of this current work is to produce an epoxy composite using a novel extraction method of Agave Americana L. To the best of our knowledge, no prior investigation has addressed the optimization of new extraction methods of Agave fibers after burial in soil for composite production. In this method, agave leaves are buried in the soil to leverage the activities of soil microorganisms, decomposing the natural matrix bound in the fibers. To assess the effectiveness of the composite, various mechanical, physical, and morphological properties, such as flexural test, density (experimental and theoretical), void fraction, water absorption, scanning electron microscope (SEM), and elemental dispersive X-ray analysis (EDX), were analyzed.

2. Materials

2.1 Preparation of RF

After harvesting, the leaves are washed in water. The fibers are separated manually and then washed in distilled water to remove unwanted substances from the fiber surface. Finally, the fiber bundles are oven dried at 70°C for 24 hours to remove moisture (Fig. 1.b). The aim of this extraction process is to obtain technical fibers in their original raw state.

2.2. Preparation of BF

Following the harvesting process, the treatment protocol is applied which consist on removing the thorns and burying the Agave leaves under a layer of soil. This method rests on the activity of microorganisms in the soil, the combined action of sun and rain favoring the development of microorganisms capable of decomposing the binding natural matrix between the fibers(De et al. 2012). The burying protocol could remain until 45 days. Once this period is finished, the fibers are separated manually. Then, the fibers obtained are washed 4 to 5 times in distilled water in order to remove any remaining unwanted materials from the fiber surface. Finally, the fiber bundles are dried in the oven at 70°C during 24 hours to remove completely the moisture (Fig. 1.c).

2.3. Matrix preparation

The epoxy resin utilized in this research is CRYSTIC VE671, a thermosetting polymer that undergoes curing when mixed with a hardener. This type of epoxy resin is commonly employed in the fabrication of fiber-reinforced composites. It is known for its versatility and is suitable for various applications. The density of CRYSTIC VE671 typically ranges between 1.04 to 1.06 g/cm^3, making it a suitable choice for composite materials where both strength and lightweight characteristics are desired.

2.4. Preparation of specimen.

The fiber bundles were cut into lengths ranging from 125 to 630 microns. Subsequently, the fibers were weighed based on their density to determine the precise amount needed to reinforce the epoxy composite. A rectangular aluminum plate mold measuring 160x120x4 mm^3 was employed for the molding process. A layer of PVA was applied to the mold to facilitate the ejection of the final composite plate. Two types of plates were produced: RF (raw fiber) and BF (biological fiber) plates, each reinforced with three different weight contents (0%, 10%, and 20%). These molded composites were cured for 24 hours at room temperature. The fabrication process and the flexural test machine setup are illustrated in Fig. 1.

2.4. Flexural test

As depicted in Fig. 1.j, the flexural test was conducted using the three-point bending method in accordance with ASTM D790-07 standards. A WDW-5 Universal Electromechanical Testing Machine was employed to perform the experiments at a temperature of 20°C, with a cross-head speed set at 2 mm/min. The dimensions of the specimen plate were 80x10x4 mm^3. Four specimens were tested, and the average of the results was calculated, as shown in Fig. 1.h.

2.5. Density

The density of the fibers was determined using a pycnometer filled with ethanol as the immersion liquid. Initially, the fibers were dried in an oven at 70°C for 24 hours to eliminate any moisture content. Subsequently, they were cut into small pieces and placed in the pycnometer. Prior to conducting the experiment, the fibers were soaked in a vessel filled with ethanol for 2 hours to eliminate any micro bubbles.

The density was calculated using the following equation:

$$\varvec{\rho}_{\varvec{f}} = \frac{\left(\varvec{m}_3 - \varvec{m}_1\right)}{\left[\left(\varvec{m}_2 - \varvec{m}_1\right) - \left(\varvec{m}_4 - \varvec{m}_3\right)\right]}\rho_e$$

1

Where ρe is the density of ethanol at 25°C, m_1 is the mass of the empty pycnometer, m_2 is the mass of the pycnometer filled with ethanol at 25°C, m_3 is the mass of the pycnometer filled with chopped fibers and m_4 is the mass of the pycnometer filled with chopped fibers and ethanol at 25°C. Same processes and equation to calculate the composite density ρ_{exp}.

But, the difference is the liquid of immersion (distilled water). Theoretical density is calculated asfollow:

$$\frac{1}{\varvec{\rho}_{\varvec{t}}} = \frac{\varvec{w}_{\varvec{f}}}{\varvec{\rho}_{\varvec{f}}} + \frac{\varvec{w}_{\varvec{m}}}{\varvec{\rho}_{\varvec{m}}}$$

2

Where, w_f and w_m are weight fractions of fiber and neat matrix, respectively in the developed composite. ρ_f and ρ_m are densities of fiber and neat matrix, respectively used in the fabrication of composite.

Void fraction content was calculated following the Eq. (3):

$$\varvec{V}\varvec{o}\varvec{i}\varvec{d}\varvec{f}\varvec{r}\varvec{a}\varvec{c}\varvec{t}\varvec{i}\varvec{o}\varvec{n}\,(\varvec{\%}) = \frac{\varvec{\rho}_{\varvec{}}}{}$$

3

2.6. Water absorption

The water absorption of the elaborated composites plates was determined. The specimens were dried in an oven at 50°C for 24 hours and cooled in desiccators. Then, the samples were immersed in distilled water and its weight were measured and controlled every day up to 18 days. The water absorption of the composites was computed by applying the following equation:

$$\varvec{W}\varvec{a}\varvec{t}\varvec{e}\varvec{r}\varvec{a}\varvec{b}\varvec{s}\varvec{o}\varvec{r}\varvec{p}\varvec{t}\varvec{i}\varvec{o}\varvec{n}\,(\varv$$

4

2.7. SEM

The observation of the microstructure of the fibers was conducted using the Scanning Electron Microscope (SEM) Thermo Scientific Q250 (TS Quinta 250).

3. Results and discussion

3.1. Flexural test

The effect of extraction methods and fiber contents (0%, 10%, and 20%) on the flexural strength and modulus of the epoxy composites is summarized in Table 1. The mechanical properties investigated include the flexural strength and modulus of the neat epoxy composites, which are reported as 137.61 MPa and 5489 MPa, respectively. Upon the addition of RF and BF, there is a consecutive increase in both flexural strength and modulus of the epoxy composites for 10% and 20% fiber contents. As shown in Table 1, it is evident that the flexural strength of RFE20 and BFE20 composites is significantly higher by approximately 16.21% and 17.66%, respectively, compared to neat epoxy. RFE10 and BFE10 exhibit a slight increase in flexural strength compared to the neat epoxy, with values of 139.4 MPa and 144.74 MPa, respectively. This slight increase can be attributed to the poor dispersion of fibers in the polymer matrix.

Table 1
Comparison of Mechanical properties of Agave reinforced with epoxy fiber.

Weight content of fiber (%)	Rm(MPa)	E(MPa)
Epoxy pur (0)	137,61 ± 24,3	5489,5 ± 302,77
RFE 10	139,4 ± 10,89	8045,67 ± 339,79
BEF 10	144,74 ± 9,32	8902 ± 289,65
RFE 20	159,93 ± 3,01	12251,33 ± 201,87
BFE 20	161,92 ± 2,3	13674 ± 130,55

The notable improvement in flexural strength for BFE 20% composites compared to RFE 20% can be attributed to the removal of non-cellulosic compounds from the BF fibers (the content of hemicelluloses was 17% and 21.05% of BF (Mansouri et al. 2020) and RF, respectively), resulting in better interfacial compatibility between BF and the epoxy matrix (Rizal et al. 2018).

The enhanced compatibility and dispersion in the composites result in better stress transferability within the material. This improvement leads to a significant enhancement in the flexural modulus of the epoxy composites. Specifically, there is an increase of 46.56%, 62.16%, 123.17%, and 149.09% in the flexural modulus for RFE10, BFE10, REF20, and BFE20, respectively, compared to the neat epoxy.

Table 1 clearly indicates that both the flexural strength and modulus increase with an increasing agave fiber content of 20%. This observation aligns with findings from Gupta et al. and Arthanarieswaran et al., who also reported that mechanical properties improved with higher fiber content in the matrix (Arthanarieswaran et al. 2016; Gupta and Srivastava 2016). Specifically, the modulus of RFE20 and BFE20 surpassed the modulus of epoxy composites loaded with 20% jute (7.37 GPa), bamboo/epoxy (4.91 GPa) (Kai Zhang, Fangxin Wang, Wenyan Liang, Zhenqing Wang 2018), and Acacia leucophloea/epoxy (4.41 GPa) (Arthanarieswaran et al. 2016) (Arthanarieswaran et al., 2016).

Composites with agave fibers enhance the performance of BF compared to RF due to the extraction method, which enhances the interfacial adhesion between the fiber and the matrix. This method also enables better resin penetration into the fiber bundle during the manufacturing process. Additionally, the increased resin penetration into the extracted fiber reduces the likelihood of fiber detachment, debonding, or extraction. These outcomes minimize the occurrence of voids or porosities at the fiber-matrix interface, resulting in improved bonding of the fiber-reinforced composite. While the cellulose content of the fibers does influence the composite properties, the enhanced performance can primarily be attributed to the improvement in fiber/matrix interaction. These observations corroborate previous findings discussed by Haddar et al. (Haddar et al. 2018).

Further evidence supporting this assertion will be provided in the SEM observation section. The impact of extraction methods on fibers and their influence on the mechanical properties of polymers have been elucidated. It has been observed that impurities and wax on the fiber surface are removed through biological extraction, thereby enhancing the interfacial adhesion between the fiber and the matrix.

3.2. Water absorption

The water absorption behavior of neat epoxy, RFE10, BFE10, RFE20, and BFE20 composites with 10% and 20% weight fibers of agave content was investigated over a 24-day period, as illustrated in Fig. 2. Neat epoxy exhibited continuous water uptake until 8 days, while the composites showed continuous absorption until 11 days for RFE10 and BFE10, and until 16 days for RFE20 and BFE20. After 1 hour, all samples displayed less than 0.1% water absorption (Fig. 2b). However, sudden increases in water absorption were observed at 1 day, with the end of the absorption period at 8, 11, and 16 days for composites with 0%, 10%, and 20% fiber content, respectively.

Notably, the neat epoxy demonstrated lower water absorption compared to the four composite types. RFE10 and RFE20 exhibited significantly higher water absorption than BFE10 and BFE20, which can be attributed to the higher amount of non-cellulosic (hemicellulose) materials in RF fibers. These fibers contain (-OH) groups capable of binding with water, along with capillary pores within the fiber structure.

Furthermore, this phenomenon is attributed to the infiltration into the free spaces caused by micro-voids and other morphological defects (Rahman et al. 2012), and/or experimental defects during the manufacturing process of the composites. The saturated water weight for neat epoxy, RFE10, BFE10, RFE20, and BFE20 composites was recorded as 1.68, 4.24, 3.98, 5.76, and 5.48, respectively.

3.3. Density

The primary advantage distinguishing cellulosic fibers from synthetic fibers is their low density, with lignocellulosic fibers typically having a density of around 1.49 g/cm^3 (Belouadah et al. 2015), compared to 2500 kg/m^3 for glass fibers (Maheshwaran et al. 2017). Cellulose fibers contain pores and voids, which contribute to their porous nature and consequently, their low density. This characteristic makes cellulose fibers suitable for reinforcement in a polymer matrix. The density of RF and BF, determined using a pycnometer, is approximately 1.23 and 1.36 g/cm3, respectively.

The loss of non-cellulosic compounds in the treated fibers (BF) results in an increased density of these fibers [33]. Both types of fibers exhibit higher density compared to other natural fibers such as Furcraea foetida (0.778 g/cm3) [34], and Sansevieria ehrenbergii (0.887 g/cm3) [35], but less than Lygeum spartum (1.49 g/cm3) [31] and Cissus quadrangularis root fiber (1.51 g/cm3) [36]. The variation in density among cellulose fibers can be attributed to various factors including climatic conditions, plant growth, plant tissue, extraction process [35], and the porosity of the microstructure [31].

Table 2 presents the experimental density, theoretical density, and void fraction (in percent) of the composites. The experimental densities of RFE10, BFE10, RFE20, and BFE20 are 1.026, 1.039, 1.041, and 1.071 g/cm3, respectively. Notably, the density of the composite is higher than that of pure epoxy (1.018 g/cm3), indicating good contact between the two phases, which reduces voids and defects, thereby increasing the density of the composites. This hypothesis of void reduction is supported by the calculation of the void fraction. The surface of the fiber plays a crucial role in facilitating interaction between the fiber and the matrix. Epoxy resin can penetrate into the voids and cracks on the surface of the biological fibers, enabling mechanical locking of the epoxy matrix onto the surface of the treated agave fibers. This results in a strong bond between the biological fiber and the epoxy matrix, leading to improved mechanical properties. Theoretical and experimental densities of the developed composites are compared in Table 2. The difference between the experimental and theoretical densities is attributed to the presence of voids in the composites.

Table 2
Comparison between Experimental density, Theoretical density and void fraction content of composite.

	Experimental density (g/cm3)	Theoretical density (g/cm3)	Void fraction content (%)
Neat Epoxy	1,018	1,04	2,11
RFE10	1,026	1,056	2,84
BFE10	1,039	1,065	2,44
RFE20	1,041	1,073	2,98
BFE20	1,071	1,091	1,83

Some voids and pores were observed in the composites due to air entrapment and moisture absorption during the manufacturing process (Fiore et al. 2015; Rajiv Kumara 2018). able 2 indicates minimal changes in density. At 10 wt% fiber content, the void fraction of RFE10 (2.84%) is higher than that of BFE10 (2.44%). Even with the addition of 20 wt% fibers, there is a notable deviation in the void fraction of RFE20 and BFE20, which are 2.98% and 1.83%, respectively. The presence of voids in RFE20 is clearly visible in the SEM image. The void fraction of the four types of composites in this study is relatively low compared to other composites. For instance, the void fraction of epoxy reinforced with 10% and 20% Ramie fibers is reported as 8.18% and 6.67%, respectively (Rajiv Kumara 2018). Similarly, the void ratio for epoxy reinforced with 12% and 24% jute content is 5.32% and 5.02%, respectively (Mishra and Biswas 2013). A higher void content in the composite indicates inadequate resin encapsulation of the fibers, resulting in cracks in the fibers and a wide gap between the fibers and the epoxy matrix. This ultimately leads to reduced resistance to water penetration, lower strength properties of the composites, and poor interfacial strength (Mishra and Biswas 2013; Fiore et al. 2015).

3.4. Scanning electron microscopy

Scanning electron microscopy (SEM) and EDX analysis were conducted on the composites after fracture under the flexural test. Figures 3, 4, and 5 illustrate the morphology of neat epoxy, RFE20, and BFE20. The fibers within the composites are randomly oriented.

In Fig. 5, large voids formed by fibers pulling out from the matrix are evident, indicating poor interfacial adhesion of the RFE20. This poor adhesion likely contributes to the disturbed mechanical properties observed in RFE20. The significant deviation in mechanical properties (flexural strength and flexural modulus) further confirms this observation for RFE20. The fracture of Agave fibers BFE20 shows reductions in the number of voids, indicating better adhesion of randomly oriented Agave epoxy composites, which contributes to its high strength under bending loads. Figure 4 illustrates the excellent bonding interface resulting from increased interaction between the fibers and the matrix, attributed to the reduction of cellulosic compounds and the formation of molecular hydrogen bonds between the fibers and the matrix. The fracture of the fibers suggests that they remain intact with the matrix, indicating improved bonding between the fiber and the matrix. The SEM micrographs in Fig. 4 also show a reduction in fiber diameter of the biological fibers, which is beneficial for mechanical properties. Both fiber diameter and length positively influence the mechanical properties. The EDX spectra of the undiluted epoxy, BFE20, and RFE20 are depicted in Figs. 3, 4, and 5, and their analyses are presented in Tables 3, 4, and 5.

Table 3
Weight percentage of each point and global image of neat epoxy

	C	O	Al	Ca	*Total*
E(2)_pt1	64.71	32.64	2.64		**100**
E(2)_pt2	67.01	30.36	1.22	1.41	**100**
E(2)_pt3	62.46	33.09	4.45		**100**
Of spectruim	71.79	27.97	0.24		**100**

Table 4
Weight percentage of each point and global image of BFE20.

(%)	*C*	*O*	*Mg*	*Al*	*Si*	*S*	*Cl*	*K*	*Ca*	*Fe*	*Na*	*Total*
Point1	52.33	42.94			0.47	0.50	1.19		2.57			**100**
Point2	71.99	27.68					0.33					**100**
Point3	69.69	29.90					0.41					**100**
Point4	50.20	29.93		0.30	0.16			1.58	3.93	13.89		**100**
Point5	65.45	32.98	0.21	0.24	0.54		0.17	0.11	0.30			**100**
Point6	36.24	33.02			0.16				30.58			**100**
Point7	68.08	31.75					0.18					**100**
Point8	74.94	24.58		0.19			0.29					**100**
Of spectruim	**59.55**	**39.17**					**0.26**		**0.76**		**0.26**	**100**

Table 5
Weight percentage of each point and global image of BFE20.

(%)	C	O	Na	Mg	Al	Si	S	Cl	K	Ca	Cu	Total
Point 1	47.04	48.91	0.56	0.42			0.37	0.45	0.17	2.07		**100**
Point 2	68.39	31.15						0.46				**100**
Point 3	60.57	31.25									8.18	**100**
Point 4	57.52	36.72								5.76		**100**
Point 5	68.32	30.64						1.04				**100**
Point 6	49.07	47.36	0.67	0.51			0.21		0.24	1.94		**100**
Point 7	55.11	43.53								1.36		**100**
Point 8	37.64	42.58	2.01	0.20	7.15	7.08	0.11	0.29	0.51	2.42		**100**
Point 9	69.68	30.11						0.21				**100**
Of spectruim	63.78	35.40						0.25		0.57		**100**

In Tables 3, 4, and 5, significant differences in the percentage of C and O are observed. Particularly, an increase in oxygen content is noted in BFE20 compared to pure epoxy. This increase is attributed to compounds present in the fibers such as cellulose, hemicellulose, lignin, and pectin. Other elements present in small amounts, such as calcium (0.76%), chlorine (0.26%), and sodium (0.26%), likely originate from the soil after burial. The difference in elements such as C and O between BFE20 and RFE20 is attributed to the treatment of the fibers, resulting in the removal of non-cellulosic compounds.

4. Conclusion

Composites reinforced with RF and BF were fabricated and investigated, revealing notable impacts of fiber extraction methods on density, water absorption, and mechanical properties. Compared to pure epoxy, the density of the composite increased by 0.78%, 2.06%, 2.28%, and 5.2% for RFE10, BFE10, RFE20, and BFE20, respectively. Water absorption reached equilibrium after 11 days for RFE10 and BFE10, and after 16 days for RFE20 and BFE20. The higher water absorption in RFE20 and BFE20 may be attributed to the hydrophilic properties of the fibers, increased non-cellulosic compounds in the 20% fiber content, and micropores observed in the composite through scanning electron micrographs.

Mechanical property analysis revealed that the addition of RF and BF enhanced both flexural strength and modulus of the composites. Furthermore, RFE10, BFE10, RFE20, and BFE20 exhibited improved density and mechanical properties compared to pure epoxy. Surface morphology analysis via SEM indicated that BFE20 exhibited better adhesion between fibers and matrix, with less debonding, chipping, and voids compared to RFE20.

Declarations

Author contributions

AM, JBN and FH contributed to study concept and design and development of the protocol and participated in designing the evaluation; AM and FH contributed to analysis and interpretation of data and critically revised the manuscript for important intellectual content; and MBA drafted the manuscript and contributed to statistical analysis. All authors read and approved the final manuscript.

Data availability

The data that support the findings of this study are available from the corresponding author upon reasonable request.

Conflict of interest

The authors declare no conflict of interest.

Ethical approval

Not applicable.

References

1. Akin DE (2013) Linen most useful: Perspectives on structure, chemistry, and enzymes for retting flax. ISRN Biotechnology 2013:23. https://doi.org/http://dx.doi.org/10.5402/2013/186534
2. Akin DE, Condon B, Sohn M, et al (2007) Optimization for enzyme-retting of flax with pectate lyase. Industrial Crops and Products 25:136–146. https://doi.org/10.1016/j.indcrop.2006.08.003
3. Arthanarieswaran VP, Kumaravel A, Kathirselvam M, Saravanakumar SS (2016) Mechanical and thermal properties of Acacia leucophloea fiber/epoxy composites: Influence of fiber loading and alkali treatment. International Journal of Polymer Analysis and Characterization 21:571–583. https://doi.org/10.1080/1023666X.2016.1183279
4. Belouadah Z, Ati A, Rokbi M (2015) Characterization of new natural cellulosic fiber from Lygeum spartum L. Carbohydrate Polymers 134:429–437. https://doi.org/10.1016/j.carbpol.2015.08.024
5. Bessadok A, Roudesli S, Marais S, et al (2009) ETUDE ET CARACTERISATION DES FIBRES D'ALFA ET D'AGAVE MODIFIEES CHIMIQUEMENT EN VUE DE LES INCORPORER DANS UN COMPOSITE AMATRICE POLYESTER. Composites Part A: Applied Science and Manufacturing 40:184–195. https://doi.org/10.1016/j.compositesa.2008.10.018
6. Bessghaier A, Oudiani EL (2010) Contribution à l ' étude du comportement mécanique des fibres d ' agave Americana L .
7. Bezazi A, Belaadi A, Bourchak M, et al (2014) Novel extraction techniques, chemical and mechanical characterisation of Agave americana L. natural fibres. Composites Part B: Engineering 66:194–203. https://doi.org/10.1016/j.compositesb.2014.05.014
8. Bouaziz MA, Rassaoui R, Besbes S (2014) Chemical composition, functional properties, and effect of inulin from tunisian Agave americana L. Leaves on textural qualities of pectin gel. Journal of Chemistry 2014:. https://doi.org/10.1155/2014/758697
9. De D, Alsace UDEH, Tenacissima S (2012) Docteur de l'universite de haute alsace
10. el Oudiani A, Chaabouni Y, Msahli S, Sakli F (2008) Crystalline Character of Agave americana L. Fibers. Textile Research Journal 78:631–644. https://doi.org/10.1177/0040517508089757
11. Estaji S, Paydayesh A, Mousavi SR, et al (2021) Polycarbonate/poly(methyl methacrylate)/silica aerogel blend composites for advanced transparent thermal insulations: Mechanical, thermal, and optical studies. Polymer Composites 42:5323–5334. https://doi.org/10.1002/pc.26226
12. Fiore V, Bella G Di, Valenza A (2015) The effect of alkaline treatment on mechanical properties of kenaf fibers and their epoxy composites. 68:14–21
13. Gupta MK, Srivastava RK (2016) Properties of sisal fibre reinforced epoxy composite. Indian Journal of Fibre and Textile Research 41:235–241
14. Haddar M, Elloumi A, Koubaa A, et al (2018) Synergetic effect of Posidonia oceanica fibres and deinking paper sludge on the thermo-mechanical properties of high density polyethylene composites. Industrial Crops and Products 121:26–35. https://doi.org/10.1016/j.indcrop.2018.04.075

15. Henriksson G, Akin DE, Hanlin RT, et al (1997) Identification and retting efficiencies of fungi isolated from dew-retted flax in the United States and Europe. Applied and Environmental Microbiology 63:3950–3956
16. Hulle A, Kadole P, Katkar P (2015) Agave Americana Leaf Fibers. Fibers 3(1):64–75
17. Jaouadi M, Msahli S, Sakli F (2011) A study of the physical and mechanical properties of paper made from Agave americana L. fibers. Materials and Manufacturing Processes 26:567–572. https://doi.org/10.1080/10426910903124878
18. Kai Zhang , Fangxin Wang , Wenyan Liang , Zhenqing Wang ZD and BY (2018) Thermal and Mechanical Properties of Bamboo Fiber Reinforced Epoxy Composites Kai. Polymer (Korea) 33:530–536. https://doi.org/10.3390/polym10060608
19. Khan Z, Yousif BF, Islam M (2017) Fracture behaviour of bamboo fiber reinforced epoxy composites. Composites Part B: Engineering 116:186–199. https://doi.org/10.1016/j.compositesb.2017.02.015
20. Labidi K, Cao Z, Zrida M, et al (2019) Alfa fiber/polypropylene composites: Influence of fiber extraction method and chemical treatments. Journal of Applied Polymer Science 47392. https://doi.org/10.1002/app.47392
21. Maheshwaran M V, Hyness NRJ, Senthamaraikannan P, Sanjay MR (2017) Characterization of natural cellulosic fiber from Epipremnum aureum stem Characterization of natural cellulosic fiber from Epipremnum aureum stem. Journal of Natural Fibers 15(6):789–798. https://doi.org/10.1080/15440478.2017.1364205
22. Mansouri A, Ben Nasr J, Ben Amar M, Elhalouani F (2020) Characterization of Fiber Extracted from Agave americana after Burial in Soil. Fibers and Polymers 21:724–732. https://doi.org/10.1007/s12221-020-8666-9
23. Mishra V, Biswas S (2013) Physical and Mechanical Properties of Bi-directional Jute Fiber epoxy Composites. Procedia Engineering 51:561–566. https://doi.org/10.1016/j.proeng.2013.01.079
24. Mousavi SR, Estaji S, Raouf Javidi M, et al (2021a) Toughening of epoxy resin systems using core–shell rubber particles: a literature review. Journal of Materials Science 56:18345–18367. https://doi.org/10.1007/s10853-021-06329-8
25. Mousavi SR, Faraj Nejad S, Jafari M, Paydayesh A (2021b) Polypropylene/ethylene propylene diene monomer/cellulose nanocrystal ternary blend nanocomposites: Effects of different parameters on mechanical, rheological, and thermal properties. Polymer Composites 42:4187–4198. https://doi.org/10.1002/pc.26137
26. Msahli S, Ydrean J, Sakli F (2005) Evaluating the Fineness of Agave Americana L. Fibers. Textile Research Journal 75(7):540–543. https://doi.org/10.1177/0040517505053808
27. Mylsamy K, Rajendran I (2011a) The mechanical properties, deformation and thermomechanical properties of alkali treated and untreated Agave continuous fibre reinforced epoxy composites. Materials and Design 32:3076–3084. https://doi.org/10.1016/j.matdes.2010.12.051
28. Mylsamy K, Rajendran I (2011b) Influence of alkali treatment and fibre length on mechanical properties of short Agave fibre reinforced epoxy composites. Materials and Design 32:4629–4640. https://doi.org/10.1016/j.matdes.2011.04.029
29. Pickering KL, Efendy MGA, Le TM (2016) Composites : Part A A review of recent developments in natural fibre composites and their mechanical performance. 83:98–112. https://doi.org/10.1016/j.compositesa.2015.08.038
30. Rahman WA, Nur S, Sudin A, Din SN (2012) Physical and mechanical properties of Pandanus amaryllifolius fiber reinforced low density polyethylene composite for packaging application. . In 2012 IEEE Symposium on Humanities, Science and Engineering Research 345–349
31. Rajiv Kumara AA (2018) Fabrication and mechanical characterization of Indian ramie reinforced polymer composites
32. Razavi M, Sadeghi N, Jafari SH, et al (2022) Thermo-rheological probe of microstructural evolution and degradation pathway in the flame-retarded PP/EVA/NOR/clay nanocomposites. Rheologica Acta 61:25–47. https://doi.org/10.1007/s00397-021-01309-w
33. Rizal S, Ikramullah, Gopakumar DA, et al (2018) Interfacial compatibility evaluation on the fiber treatment in the Typha fiber reinforced epoxy composites and their effect on the chemical and mechanical properties. Polymers 10:. https://doi.org/10.3390/polym10121316
34. Rosli NA, Ahmad I, Abdullah I, et al (2015) Hydrophobic modification of cellulose isolated from Agave angustifolia fibre by graft copolymerisation using methyl methacrylate. Carbohydrate Polymers 125:69–75. https://doi.org/10.1016/j.carbpol.2015.03.002
35. Singha AS, Rana RK (2012) Natural fiber reinforced polystyrene composites: Effect of fiber loading, fiber dimensions and surface modification on mechanical properties. Materials and Design 41:289–297. https://doi.org/10.1016/j.matdes.2012.05.001

Figures

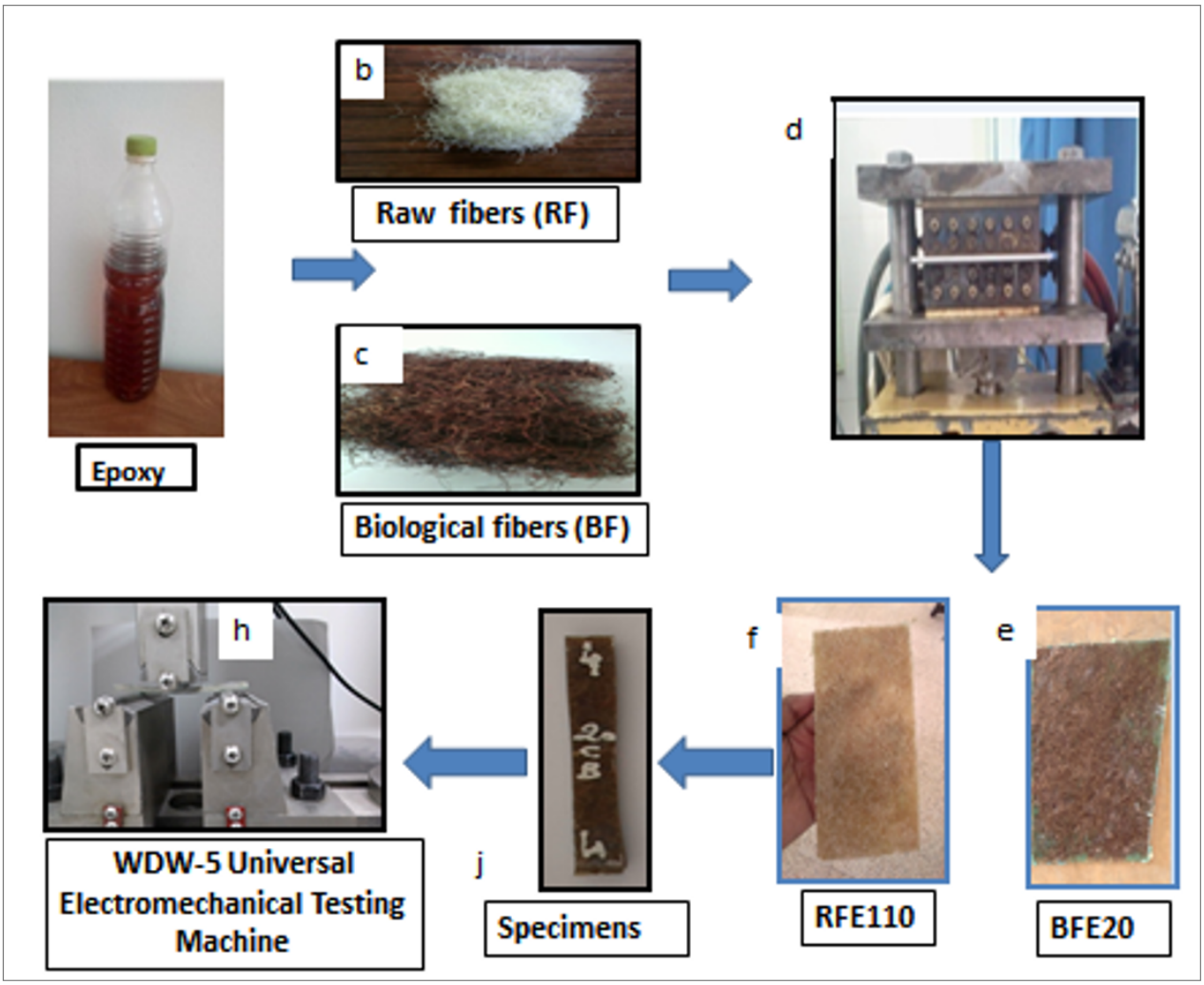

Figure 1

The fabrication process of the composite and the flexural test machine.

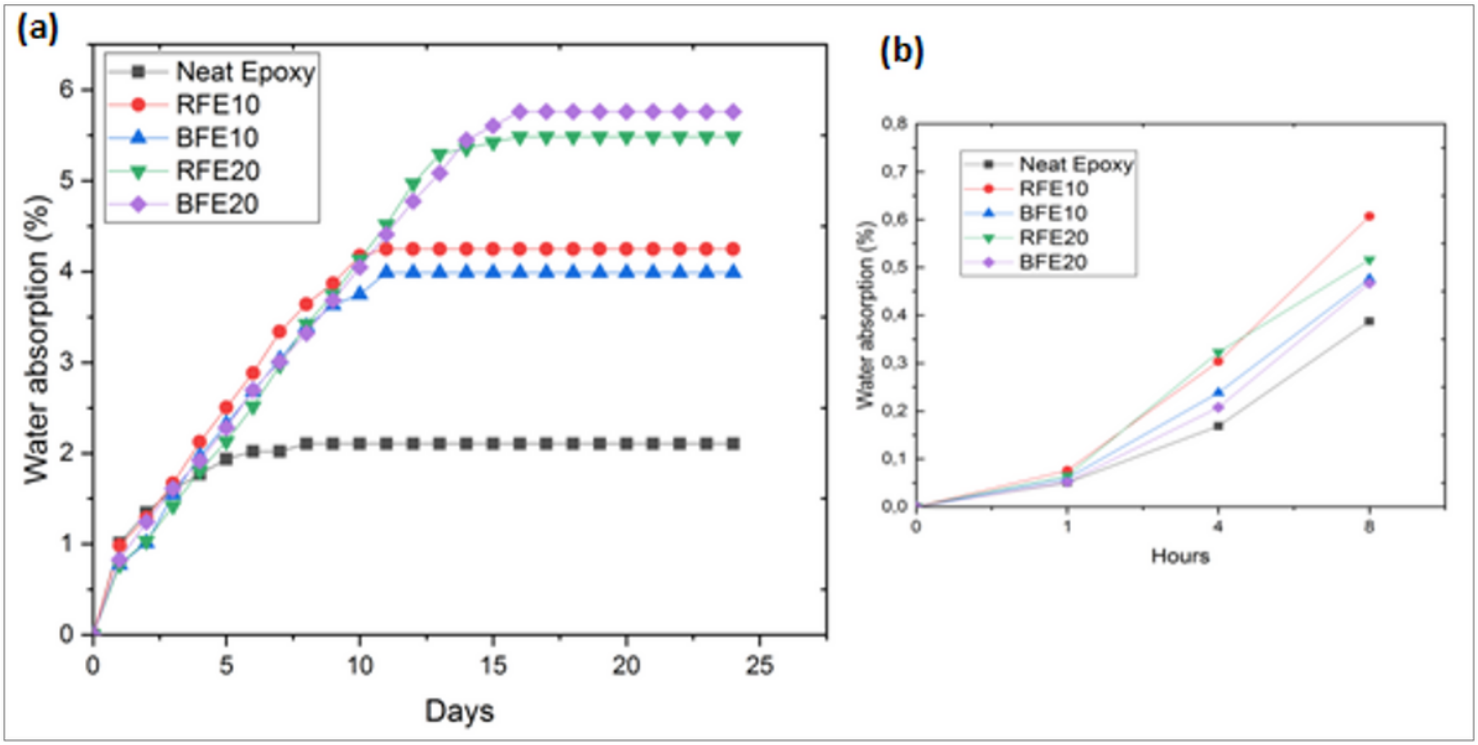

Figure 2

(a) Composites water absorption vs. days; (b) composites water absorption vs. hours.

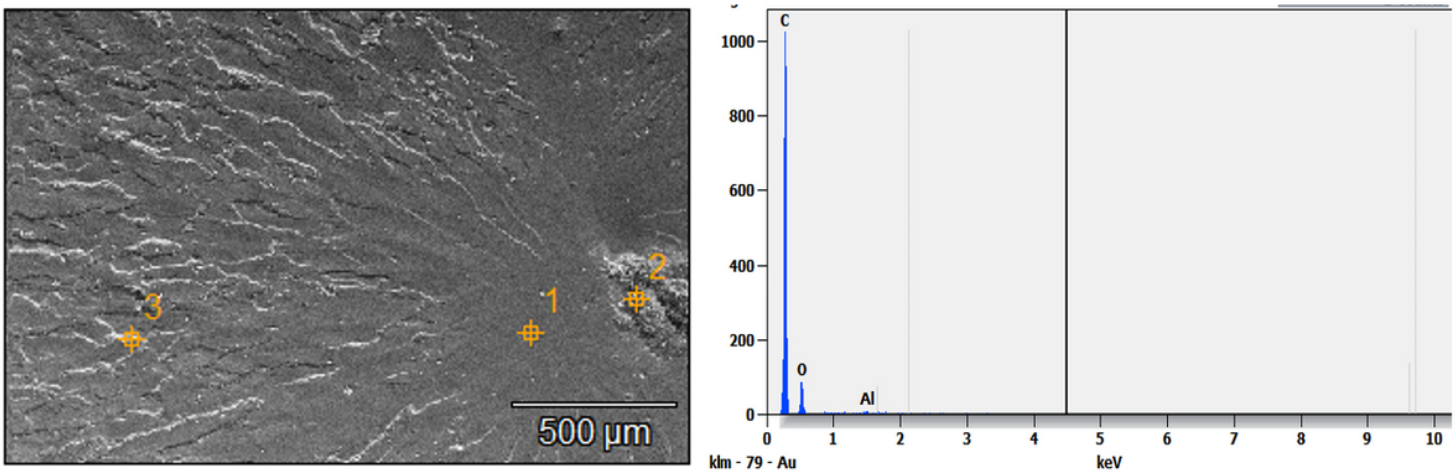

Figure 3

SEM analysis EDX analysis of neat epoxy.

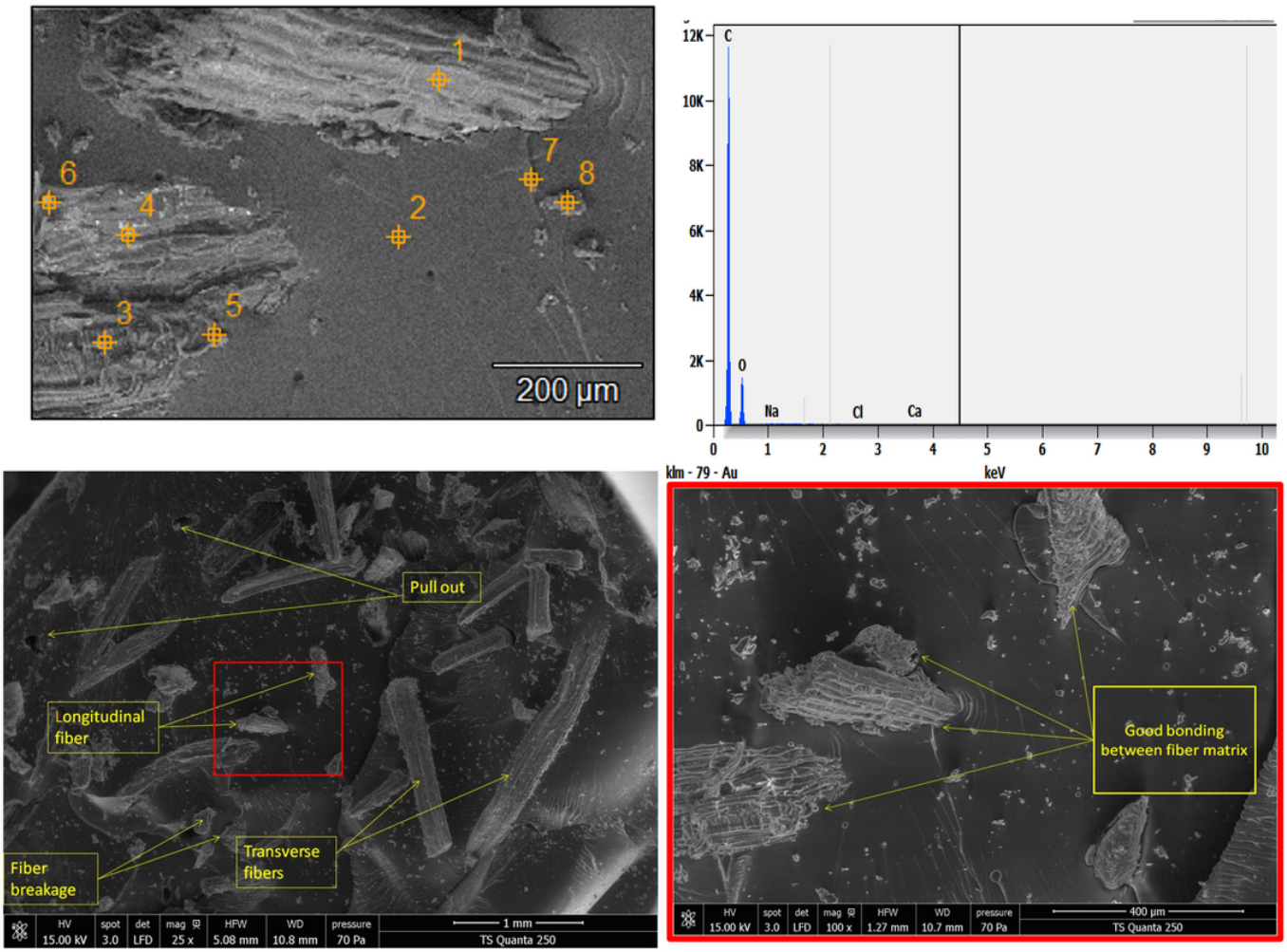

Figure 4

SEM analysis and EDX analysis of BFE20.

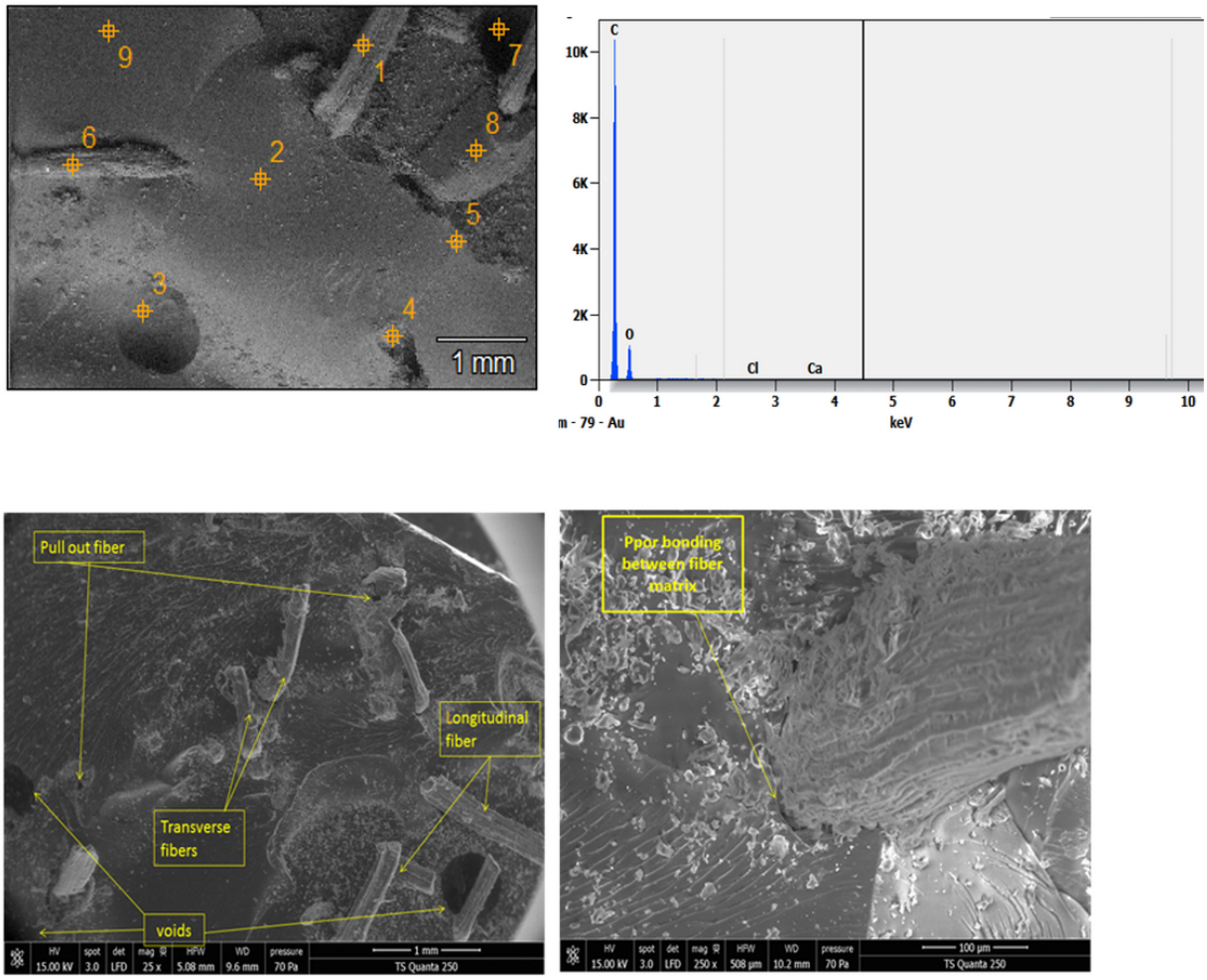

Figure 5

SEM analysis and EDX analysis of RFE20.